

# The Surface Analysis Toolbox:

## Exploring the fusion of surface-sensitive techniques for comprehensive sample understanding



### Introduction

As the demand for high-performance materials increases, so does the importance of surface engineering. A material's surface is the point of interaction with the external environment and other materials; therefore, many of the problems associated with modern materials can be solved only by understanding the physical and chemical interactions that occur at the surface or at the interfaces of a material's layers. The surface will influence such factors as corrosion rates, catalytic activity, adhesive properties, wettability, contact potential, and failure mechanisms. Surface modification can be used to alter or improve these characteristics, and so surface analysis is used to understand the surface chemistry of a material and investigate the efficacy of surface engineering. From non-stick cookware coatings to thin-film electronics and bio-active surfaces, X-ray photoelectron spectroscopy (XPS) is one of the standard tools for surface characterization.

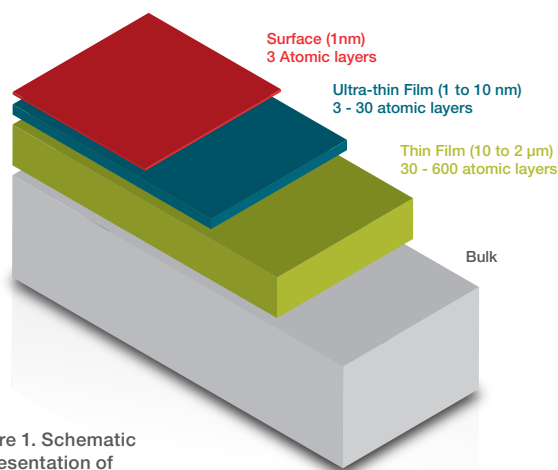


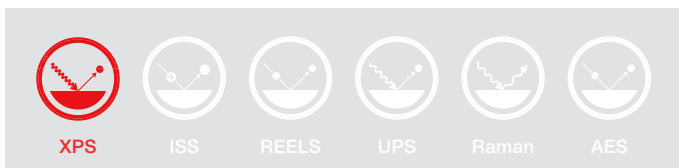
Figure 1. Schematic representation of material surface.

A surface layer (see Figure 1) is defined as being up to three atomic layers thick (~1 nm), depending upon the material. Layers up to approximately 10 nm are considered ultra-thin films, and layers up to approximately 1  $\mu\text{m}$  are thin films. The remainder of the solid is referred to as bulk material. This terminology is not definitive, however, and the distinction between the layer types can vary depending upon the material and its application. The surface represents a discontinuity between one phase and another; therefore, the physical and chemical properties of the surface are different from those of the bulk material. These differences affect the topmost atomic layer of the material to a large extent. In the bulk of the material, an atom is surrounded on all sides in a regular manner by atoms composing that material. Because a surface atom is not surrounded by atoms on all sides, it has bonding potential, which makes the surface atom more reactive than atoms in the bulk.

X-ray photoelectron spectroscopy is a key technique for surface chemical analysis, and since it became a commercially available technique over fifty years ago, it has become established as one of the core technologies for understanding materials. In that time, other experimental techniques have been added to instruments to further understanding of additional properties of the material under investigation.

In this paper, we will introduce X-ray photoelectron spectroscopy and the related techniques that can be added to support XPS analysis to understand surface chemistry.





### X-ray photoelectron spectroscopy

X-ray photoelectron spectroscopy (XPS), also known as electron spectroscopy for chemical analysis (ESCA), is a technique for analyzing the surface chemistry of a material. XPS can measure the elemental composition, empirical formula, chemical state, and electronic state of the elements within a material. XPS spectra are obtained by irradiating a solid surface with a beam of X-rays while simultaneously measuring the kinetic energy and electrons that are emitted from the top 1–10 nm of the material being analyzed. A photoelectron spectrum (see Figure 2, for example) is recorded by counting ejected electrons over a range of electron kinetic energies. Peaks appear in the spectrum due to atoms emitting electrons of a characteristic energy. The energies and intensities of the photoelectron peaks enable identification and quantification of all surface elements (except hydrogen and helium).

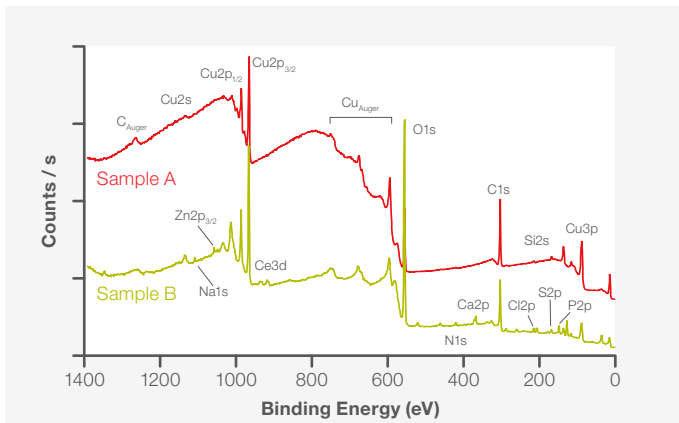
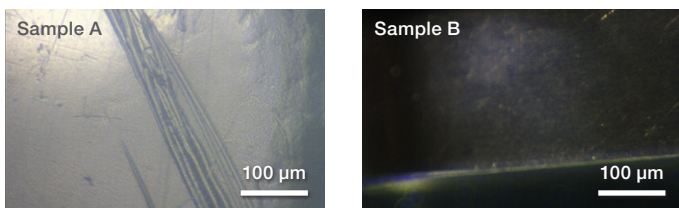


Figure 2. XPS elemental survey spectra from two different copper samples, with atomic % (At%) quantification.

In the example shown in Figure 2, two different copper samples were analyzed using XPS. Wide energy scanned XPS survey spectra are shown for each sample. The different peaks in each spectrum identify different elements on the sample surfaces; e.g., the surface of sample B also includes cerium and phosphorus. The elemental atomic percent quantification (At%) for each sample is also shown. In both samples, because there is a significant amount of carbon adsorbed from the atmosphere onto the surface, and XPS is a very surface sensitive technique, the carbon At% is reasonably high. As we will see, XPS instruments have methods available to remove this “adventitious” carbon layer to further investigate the surface beneath.

Element	At% Sample A	At% Sample B
Si	3.2	2.2
P	-	3.3
S	-	0.7
Cl	1.5	2.1
C	61.1	28.0
Ca	-	1.3
N	-	2.0
O	25.8	52.3
Ce	-	0.3
Cu	8.5	6.7
Zn	-	0.2
Na	-	1.0

Because photoelectrons can travel only a short distance in matter (0–10 nm) before losing energy, XPS is very surface sensitive. As we have seen, XPS can be used to analyze elements in a surface. The real strength of XPS, however, is its ability to investigate the chemical bonding states of those elements. If we measure the kinetic energy of the photoelectron peaks in finer detail, then we see that even for the same element, the peak energy may shift depending on the surface chemistry. This is known as the chemical shift. The ability to detect and quantify this shift makes XPS such a powerful analytical technique.

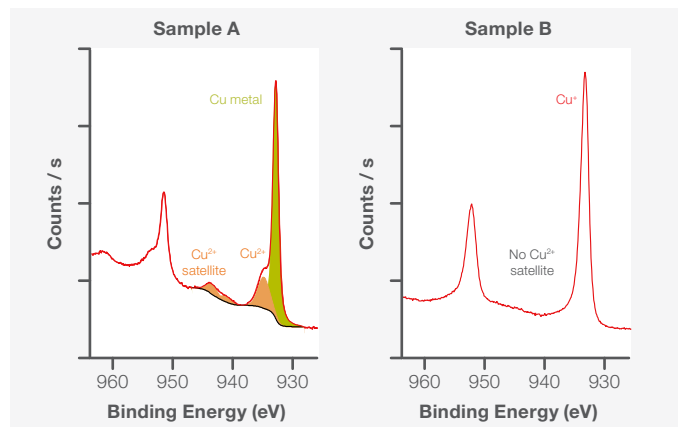


Figure 3. High energy resolution spectra showing copper chemical bonding.

In Figure 3, we see high energy resolution spectra acquired from the copper samples, A and B. The different structure observed in each spectrum indicates that the copper chemistry on each sample is different. With Sample A, for example, we see a peak due to copper metal, and we also see structure due to copper in a  $\text{Cu}^{2+}$  oxidation state, which is shifted to higher binding energy. In the oxidized bonding state, each copper electron experiences a relatively higher nuclear charge compared to metallic copper. This makes those electrons slightly harder to ionize, which manifests as a peak shift to a higher binding energy for copper oxide.

The surface specificity of XPS is particularly useful because it gives the analyst information about the part of the sample that interacts with the rest of the environment. Many modern materials, however, are composites composed of multiple layers of different elemental and chemical composition. The overall performance of these materials within their applications often depends on the interactions that occur at the interfaces between the different layers. By combining XPS with ion milling, the analyst can remove portions of the surface and use XPS to analyze the composition and chemistry of buried layers and interfaces.

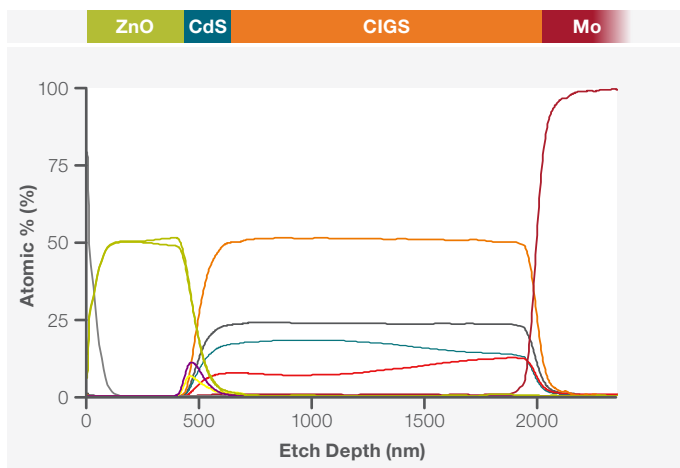


Figure 4. XPS sputter depth profile of a CIGS solar cell, with Cu2p spectra acquired during profile.

Figure 4 shows the XPS sputter depth profile for a CIGS solar cell device. The profile was created by successively acquiring XPS spectroscopic data and ion milling sub-nm portions of the surface. In this case, the total thickness of the stack was 2  $\mu\text{m}$ . With XPS, it was possible to measure the composition of the stack as a function of depth. The relative composition of the CIGS layer, for example, affects the properties of the solar cell device, changing the wavelength of the light photons that are absorbed. XPS profiling has also allowed the analyst to identify and analyze the interfacial cadmium sulphide layer that appears between the zinc oxide and CIGS layers.

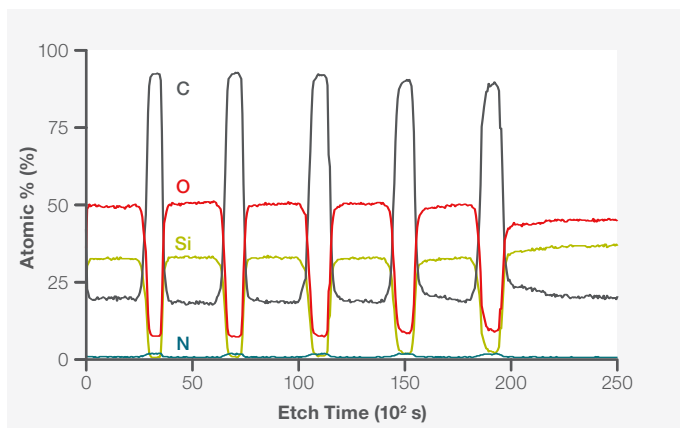
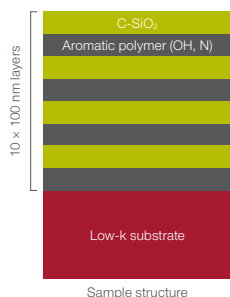


Figure 5. Small argon cluster profile through C-SiO<sub>2</sub> / aromatic polymer multilayer stack.

Another example of an XPS depth profile is shown in Figure 5. Here, the film stack is a complex mixture of inorganic and organic layers. The analyst must be careful not to damage the chemistry of the softer organic layers, while at the same time being able to efficiently sputter through the harder inorganic layers at a reasonable sputter rate. The Thermo Scientific™ MAGCIS Ion Source was used to generate a beam of small argon clusters (8 keV, Ar<sub>150</sub><sup>+</sup>), and these gas cluster ions were perfectly suited to this task. A discussion of gas cluster ion sources is beyond the scope of this paper, but links to further information on the technology and its applications can be found in the Recommended Reading section at the end.

We have seen XPS used for analyzing single points on different samples and also for measuring sample composition as a function of depth. XPS can also be used to collect elemental/chemical state information as a function of spatial coordinates, i.e., XPS imaging. Thermo Scientific XPS systems can acquire XPS images using two different data collection philosophies. First, the sample can be rastered (either rapidly or more slowly) underneath a fixed X-ray spot, collecting full XPS spectra at each pixel in the image. The data can be processed post-acquisition to generate elemental or chemical state composition maps as a function of X, Y coordinates.

Figure 6 shows an optical image of a microelectronic bond pad (200  $\mu\text{m}$  diameter) analyzed on a Thermo Scientific Nexsa™ Surface Analysis System. The white pad appears homogeneous on the optical image, with a clear darker border around the pad. The sample was imaged using the method described above, collecting silicon, tungsten, titanium, and cobalt spectra at each pixel. Where the sample is rapidly rastered underneath the X-ray spot to create a XPS SnapMap image, such images can be collected in minutes or tens of minutes, whereas in previous years, such an experiment would have taken several hours.

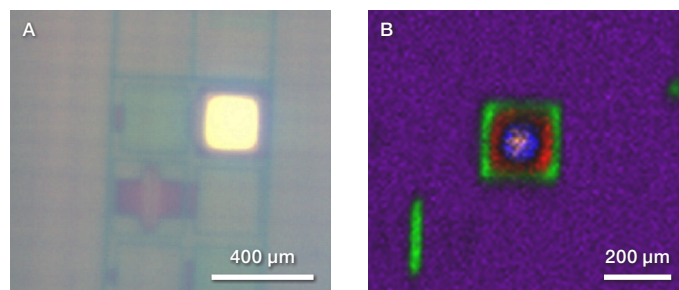


Figure 6. Nexsa XPS System optical image (A) of microelectronic bond pad, together with XPS SnapMap image (B), showing different chemical bonding states on pad.

When the XPS spectra are processed, the optically homogeneous pad is revealed to have a complex structure with a variety of chemical bonding states. The pad is bordered by tungsten oxide with two different titanium chemical states, oxide and nitride, in the middle. At the very center of the pad is some cobalt silicide. In this way, XPS provides “chemical eyes” that allow the analyst to see chemical structure that would otherwise be invisible.

A second imaging method, available on the Thermo Scientific ESCALAB™ Xi+ XPS Microprobe, uses the lens of the photoelectron detection system to preserve X, Y spatial information as the electrons leave the sample and head toward the detector. With this method, called parallel imaging, the sample stays fixed underneath a fixed X-ray spot. Figure 7 shows an example of parallel imaging of a catalyst powder. The optical image from the ESCALAB Xi+ XPS Microprobe shows some brown and some white particles. Full oxygen spectra were collected at each pixel of a parallel image, allowing an XPS image of two catalyst particles to be generated.

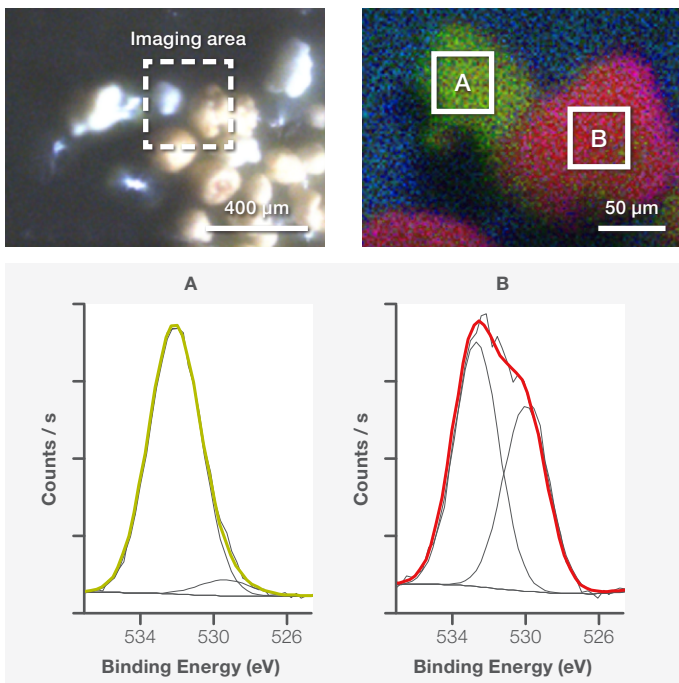
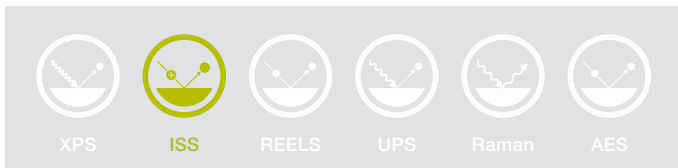


Figure 7. ESCALAB Xi+ XPS Microprobe optical image and O1s XPS parallel image of catalyst powder particles.

The green particle in the XPS image was found to be mainly silicon oxide, whereas the oxygen chemistry of the red particle is more complex, containing both silicon oxide and metal oxide bonding. The same XPS imaging analysis also included nickel and iron images, where higher concentrations of these metals correlate with the metal oxide in the O1s image.



### Ion scattering spectroscopy (ISS) (or LEIS)

Ion scattering spectroscopy (ISS) is a technique for detecting which elements are present in the top monolayer of a surface, making it even more surface sensitive than XPS. It works by firing a beam of noble gas ions (typically 1 keV He<sup>+</sup>) at the surface and measuring the kinetic energy of the ions scattered from that surface. Peaks are observed in an ISS spectrum corresponding to elastic scattering of ions from atoms in the top monolayer of the sample surface. Each element at the sample surface produces a peak at a different measured kinetic energy, caused by the momentum transfer between the incident ion and atom. The scattered ion and the scattering atom are normally of different masses, but the total momentum of the atom and ion is conserved. Therefore, as the initially “stationary” atom recoils, some kinetic energy is lost from the scattered ion, and the quantity of lost energy depends on the relative masses of the atom and probing ion. In the schematic below (Figure 8), the ISS spectrum would contain peaks from the blue and green atoms but not from the buried red atoms. Helium ions scattered from lower mass surface atoms, e.g., O or Si, are detected with a lower kinetic energy, whereas heavier surface atoms, e.g., Hf or Au, cause the ions to scatter with a higher kinetic energy.

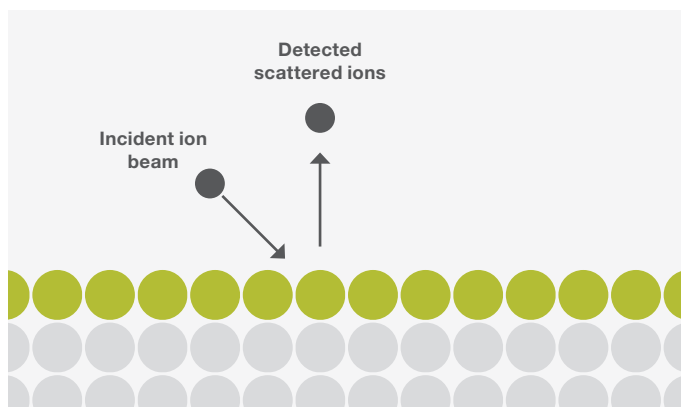


Figure 8. Schematic representation of an ISS analysis.

XPS and ISS are complementary surface analysis techniques. XPS provides elemental and chemical bonding state information from several monolayers of a surface (0–10 nm without sputtering), and, as already mentioned, ISS provides the analyst elemental information with extreme surface sensitivity. Typical application areas for XPS/ISS combined analysis are the study of ultra-thin semiconductor films, measurement of segregation in alloys or perovskites, and analysis of surface contamination. The example below (Figures 9 and 10) demonstrates the complementary information available from ISS when combined with XPS. A series of samples was created by using atomic layer deposition (ALD) to deposit increasingly thicker layers of HfO<sub>2</sub> onto an existing 1 nm SiO<sub>2</sub>/Si substrate.

XPS analysis of the samples enabled quantification of the films and an evaluation of the HfO<sub>2</sub> and SiO<sub>2</sub> layer thickness. As expected, as the number of ALD cycles increased, the total amount of HfO<sub>2</sub> deposited onto the surface increased.

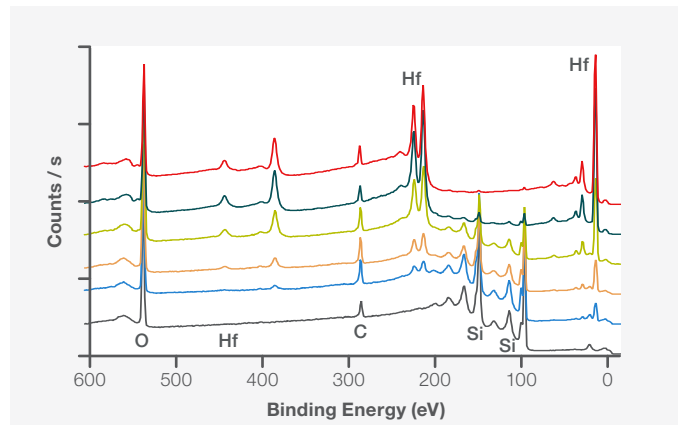
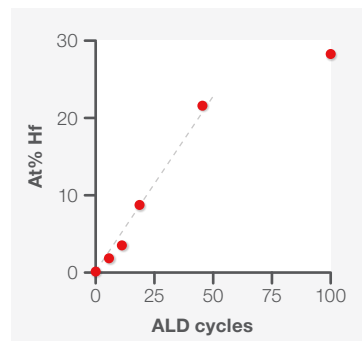


Figure 9. XPS analysis of a series of HfO<sub>2</sub> films deposited by ALD onto 1 nm SiO<sub>2</sub>/Si substrates.

It was not possible, however, to use XPS to evaluate whether the HfO<sub>2</sub> films had grown with partial coverage or whether they were completely closed. When analyzing the samples with ISS, however, if the HfO<sub>2</sub> films were



completely closed, then we would expect no signal from the SiO<sub>2</sub> underneath. If, instead, the HfO<sub>2</sub> grew as islands, then we would expect ISS to detect the SiO<sub>2</sub> between the HfO<sub>2</sub> islands. We can therefore use ISS to evaluate the coverage of the HfO<sub>2</sub> films, even though we cannot do this with XPS (see Figure 15). A silicon peak was observed in the ISS data all the way up to 20 ALD cycles, indicating the films have partial coverage up to this point. At higher numbers of ALD cycles, the silicon signal is not visible, indicating the films are closed.

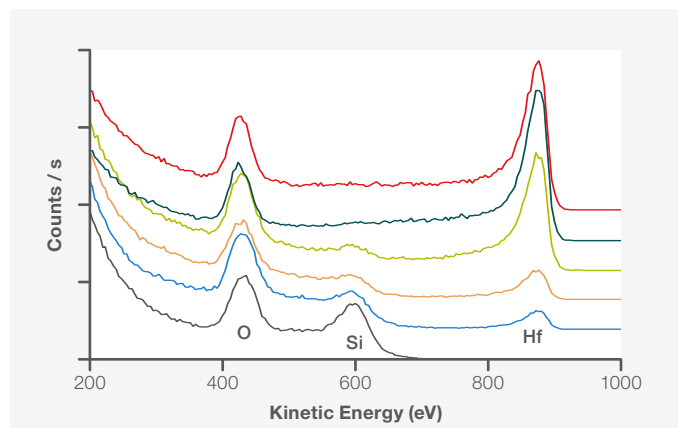
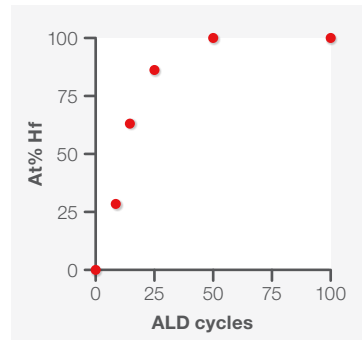


Figure 10. ISS analysis of a series of HfO<sub>2</sub> films deposited by ALD onto 1 nm SiO<sub>2</sub>/Si substrates.



Another example of combined XPS/ISS analysis makes use of the different sampling depths of each technique. A double perovskite was analyzed with XPS to identify and quantify the elements within the top 10 nm of the surface. As shown in Figure 11, the expected La, Se, Fe, and Co were observed in the XPS survey spectrum, and it was possible to quantify the atomic concentration of each.

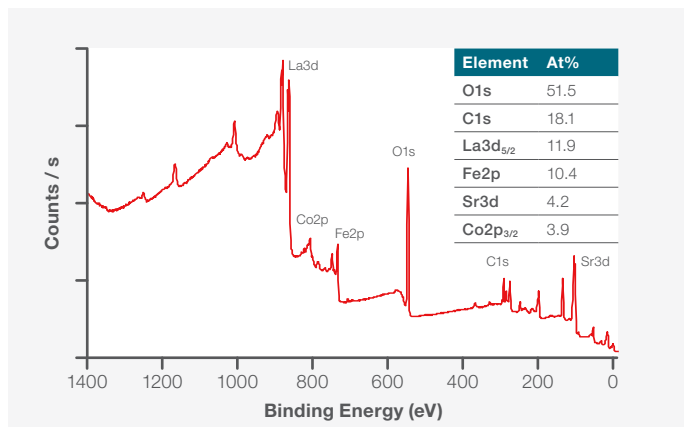


Figure 11. XPS survey spectrum of LaSrFeCoO double perovskite.

The as-received ISS spectrum from the same analysis position (see Figure 12), however, has no peak due to iron or cobalt, even though the Sr and La peaks are visible. Only after a period of argon ion sputtering does a peak due to iron and/or cobalt appear. When compared with the XPS data, the ISS analysis clearly shows that strontium and lanthanum preferentially segregate to the surface in the LaSrFeCoO double perovskite.

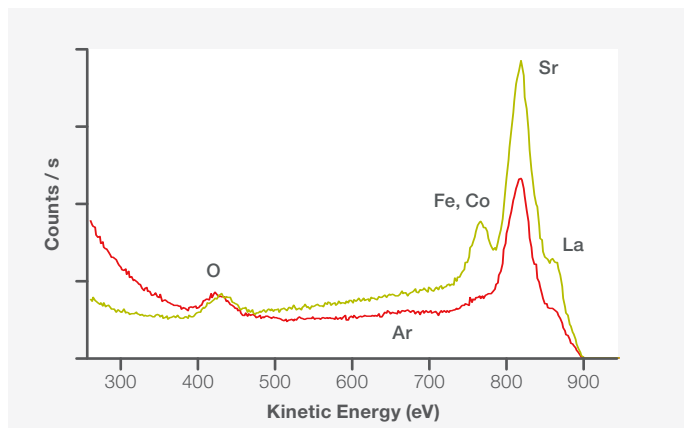


Figure 12. ISS spectra of LaSrFeCoO double perovskite as received and after ion sputtering.



### Reflected electron energy loss spectroscopy (REELS)

Reflection electron energy loss spectroscopy (REELS) operates by firing a beam of electrons at the surface and measuring the kinetic energy of the scattered electrons. It provides valence electronic information from a similar range of depths as XPS (~0–10 nm) and, in some cases, can also detect and quantify hydrogen, which XPS cannot. In the schematic shown below (Figure 13), the REELS spectrum would consist of information from several layers of the red atoms.

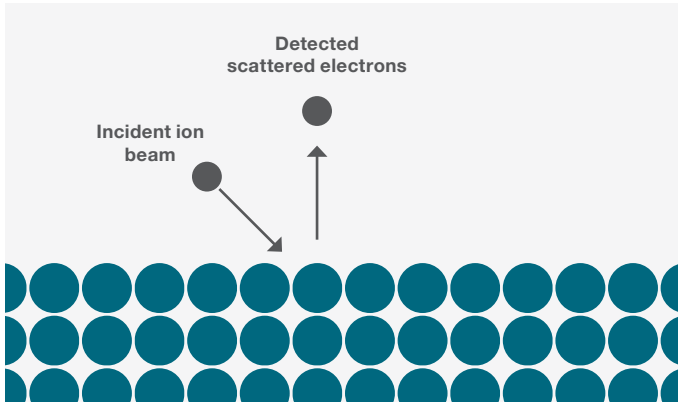


Figure 13. Schematic representation of a REELS experiment.

REELS is ideal for the analysis of metal oxides, semiconductor films, or organic materials with conjugated bonding configurations. It can measure the band gap of a metal oxide, for example, or the relative energies of the lowest unoccupied energy levels in an OLED material. REELS measurement of the band gap of the double perovskite sample discussed in the above ISS section, LaSrFeCoO, is shown below in Figure 14. A beam of 1 keV electrons was scattered from the perovskite surface. Most of those electrons reflect directly from the surface without losing any energy and are detected at a kinetic energy that is the same as the beam energy. These elastically scattered electrons form the most intense part of the REELS spectrum. They cause the strongest peak which defines the 0 eV position on the energy loss scale.

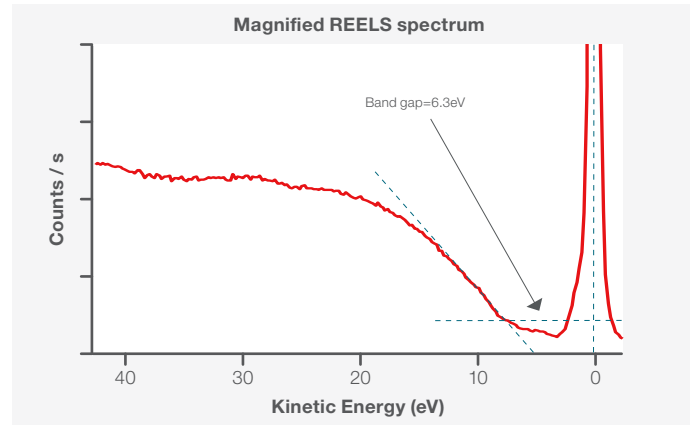
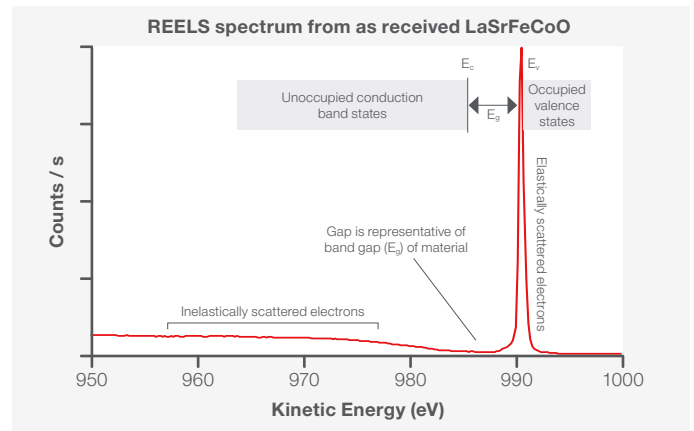


Figure 14. 1 keV REELS spectrum from the double perovskite, LaSrFeCoO, used for measuring the sample band gap.

Some other electrons from the 1 keV electron beam do interact with the surface and give up some of their energy, to promote electrons from occupied valence levels to unoccupied conduction band states, for example. The electrons scattered from the surface then have a lower kinetic energy than the initial beam and appear at a higher energy loss value in the REELS spectrum (Figure 19). Because the sample has a finite band gap, the incoming electrons cannot give up a random amount of energy to the surface; they must give up energy that is at least the equivalent of the band gap. On the REELS spectrum, this effect appears as a gap between the peak due to elastically scattered electrons and the structure due to inelastically scattered electrons (see magnified REELS spectrum in Figure 14). The Thermo Scientific Avantage Software can automatically measure the magnitude of this gap in the spectrum and return a value of the sample band gap.

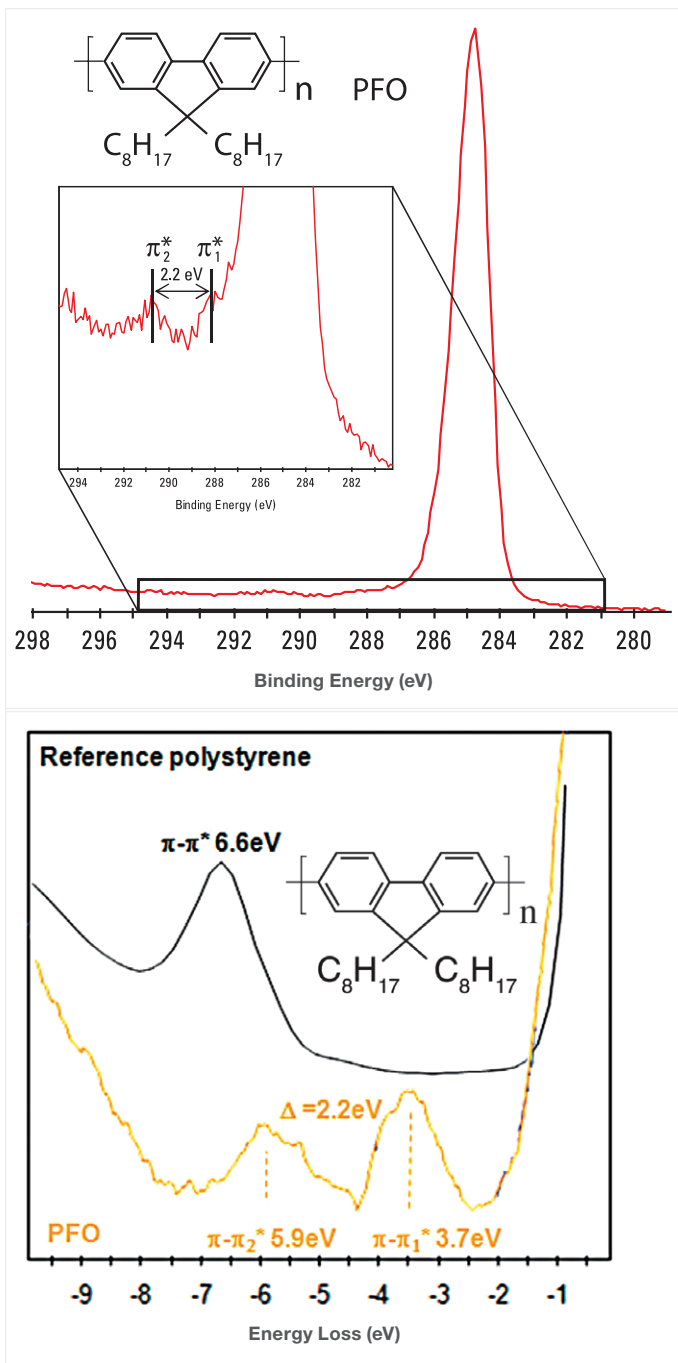


Figure 15. XPS C1s and 1 keV REELS spectrum of PFO OLED material (together with REELS spectrum of polystyrene for reference).

For materials with conjugated carbon bonding systems, XPS and REELS provide interesting complementary information. In the example shown in Figure 15, the OLED material poly(9,9-di-n-octylfluorenyl-2,7-diyl), more simply known as PFO, was analyzed with XPS and REELS. The material is composed only of carbon and hydrogen. The XPS spectrum shows the core-level peak associated with ionization from the C1s level, but closer inspection of the spectrum reveals two very weak peaks to higher binding energy. These peaks are due to the main C1s photoelectron giving up some energy to promote an electronic transition from the highest occupied molecular orbitals (HOMO) in PFO into the lowest unoccupied molecular orbitals (LUMO). The HOMO and LUMO have  $\pi$  and  $\pi^*$  character, respectively.

In the REELS spectrum from the same sample (Figure 15), the same two peaks can be identified, but they are much stronger and sharper. (The situation can also be envisaged for other samples where chemically shifted C1s peaks overlap the  $\pi$ - $\pi^*$  shake-up satellites, but this would not be a problem with REELS.) The shift of these peaks on the energy loss scale relative to the elastic peak gives the analyst a direct measure of relative energies of the HOMO and LUMO levels, and so REELS can be used to build energy level diagrams in materials such as OLEDs. As an interesting comparison, because polystyrene has a completely different bonding structure compared to PFO, we can see that the  $\pi$ - $\pi^*$  structure in a REELS spectrum is also completely different.

Another interesting capability of REELS is its ability to detect and quantify hydrogen. When analyzing a polymer, for example, XPS could be used to detect and quantify atoms such as carbon, oxygen, or nitrogen, but it cannot see the hydrogen. A combined XPS/REELS analysis, therefore, would enable a more complete compositional analysis of the polymer. 1 keV REELS was used to analyze a range of polymers; the results are shown in Figure 16. For polymers with conjugated carbon bonding, such as PET and polystyrene (PS), the  $\pi$ - $\pi^*$  shake-up features are seen, giving the HOMO-LUMO electronic information previously discussed above the PFO. Approximately 1.8 eV shifted from the primary elastic peak, most of the polymers also show a small peak due to hydrogen. (The only spectrum without this hydrogenic peak was acquired from PTFE, which has no hydrogen.)

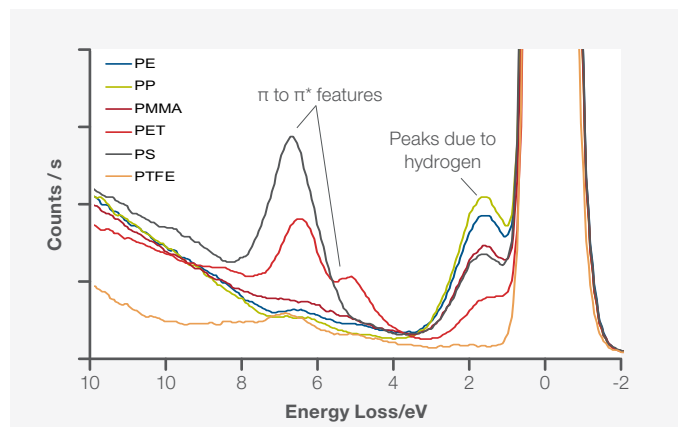
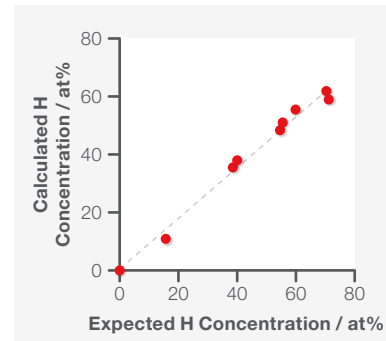


Figure 16. ESCALAB Xi+ XPS Microprobe REELS spectra of a selection of polymers.

The origin of the hydrogen peak is analogous to the ISS process, but instead of a noble gas ion scattering from a heavier element, an electron is scattering from relatively low-mass hydrogen. The primary elastic peak in the polymer analysis is composed of electrons that have scattered elastically from atoms such as carbon, oxygen, or nitrogen. When the electrons strike the hydrogen atoms, however, because the hydrogen is so much lighter, the hydrogen recoils, and a process similar to ISS takes place. The energy of the electrons scattered from the hydrogen is therefore shifted from those electrons scattered from the other atoms. The relative intensities of the hydrogen peak and the primary elastic peak are proportional to the relative amounts of hydrogen and other atoms, such as carbon, oxygen, and nitrogen. A simple peak deconvolution of the two peaks can therefore be used to quantify the hydrogen.



The primary elastic peak in the polymer analysis is composed of electrons that have scattered elastically from atoms such as carbon, oxygen, or nitrogen. When the electrons strike the hydrogen atoms, however, because the hydrogen is so much lighter, the hydrogen recoils, and a process similar to ISS takes place. The energy of the electrons scattered from the hydrogen is therefore shifted from those electrons scattered from the other atoms. The relative intensities of the hydrogen peak and the primary elastic peak are proportional to the relative amounts of hydrogen and other atoms, such as carbon, oxygen, and nitrogen. A simple peak deconvolution of the two peaks can therefore be used to quantify the hydrogen.



## UV photoelectron spectroscopy

Ultraviolet photoelectron spectroscopy (UPS) is one of the most well-known surface analysis techniques complementary to XPS. The two main applications for the technique are investigation of the valence electronic structure of surfaces and measurement of the work function or ionization potential of a sample. UPS operates on the same principles as XPS, with the main difference being that ionizing radiation is utilized at energies that are a fraction of that used for XPS. In a laboratory setting, ultraviolet photons are typically produced using a gas discharge lamp (see Figure 17), usually filled with helium. The principal photons emitted by helium gas have energies of 21.2 eV (He I) and 40.8 eV (He II). (Other gases, such as argon and neon, can also be used for UPS analysis where the choice of gas determines the energy of the UV photon.)



Figure 17. Discharge lamp used for UPS.

Since UV photons have a much lower energy than X-rays, most core-level photoemissions are not accessible using UPS, and spectral acquisition is limited to the valence band region. Additionally, UPS has a much greater surface sensitivity than even XPS, because the lower energy UV photons generate significantly lower energy photoelectrons, which have a much shorter inelastic mean free path than observed in XPS. (UPS has an approximate sample depth of 2–3 nm compared to 10 nm for XPS.) Figure 18 shows an example comparing XPS core-level spectra with UPS valence band spectra. The example is from a C<sub>60</sub> film, which initially had adventitious carbon on the surface. The XPS C<sub>1s</sub> spectrum contains a mixture of structure due to both the adventitious carbon and the underlying C<sub>60</sub> film. The as-received UPS valence band spectrum, however, because it is so much more surface sensitive, has only structure associated with the adventitious carbon. After gently sputtering the surface with argon clusters, to prevent any damage to the C<sub>60</sub> film, valence band structure to the C<sub>60</sub> becomes visible.

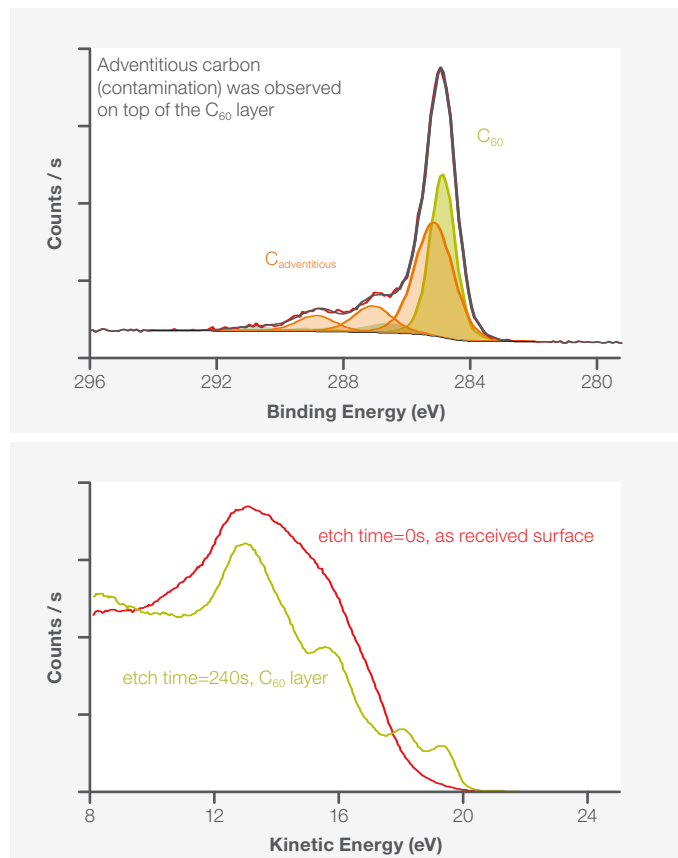


Figure 18. Core-level C<sub>1s</sub> and UPS valence band spectra for adventitious carbon and C<sub>60</sub>.

The structure in a UPS valence band spectrum reflects the occupied electronic states in the valence band of the sample. Many of the molecular orbitals from which the valence band photoelectron signal originates have a high degree of hybridization; therefore, the shifts in peak binding energy are far more varied and subtle than those observed for core-level photoemission peaks. Even though assignment of the valence band peaks is very difficult, unless the user has access to high level *ab initio* calculations, it is still possible to measure useful information. If the energy of the Fermi level is known, it is possible to measure the energy gap from that Fermi level to the leading edge of the UPS valence band structure. This energy is sometimes known as the valence band offset, and its meaning is shown schematically in Figure 19.

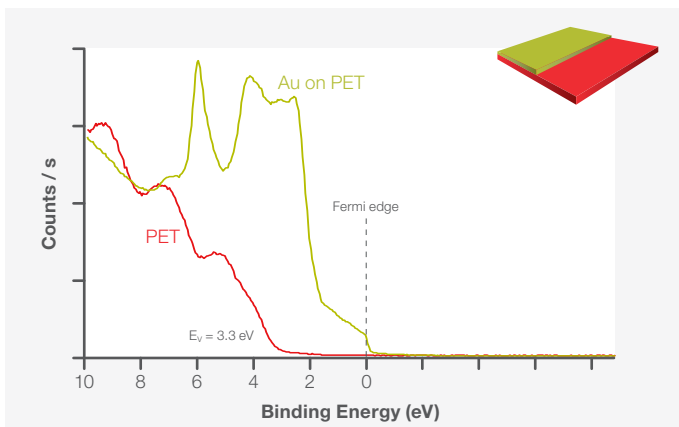
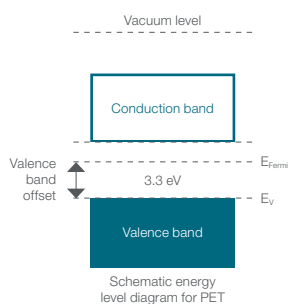


Figure 19. UPS valence band data for PET and a gold leaf in electrical connection with the PET.

The UPS valence band spectrum from a polyethylene terephthalate (PET) sample is shown in Figure 10. PET is obviously an insulator, and when the UPS spectrum is acquired, it is not possible to observe any structure at energies near the Fermi level.



In order to measure the Fermi edge position, a gold leaf was mounted on top of the PET sample in electrical contact. The UPS valence band spectrum from the gold sample has a clear Fermi edge. If we assume good electrical contact between the samples, it is possible to assume that the gold Fermi edge position is now the same as that of the PET. The energy separation between the leading edge of the PET valence band structure and the gold Fermi edge can then be measured to yield the valence band offset of PET ( $E_V=3.3$  eV).

If we can measure the energy difference between the Fermi level and the vacuum level, then we can measure the sample work function. The work function is a useful material property to know, for example, during the development of electronic devices, where matching of valence and conduction bands in multi-layered devices is required. The work function is derived spectroscopically by measuring the energy difference between the Fermi level and the cut-off, which is where the spectroscopic structure finishes at low kinetic energy. Measuring the work function for a gold sample is shown in Figure 20, where the Fermi level and spectrum cut-off are marked. (It is necessary to apply a small, negative bias voltage to the sample, e.g., -5 V, when measuring the work function.)

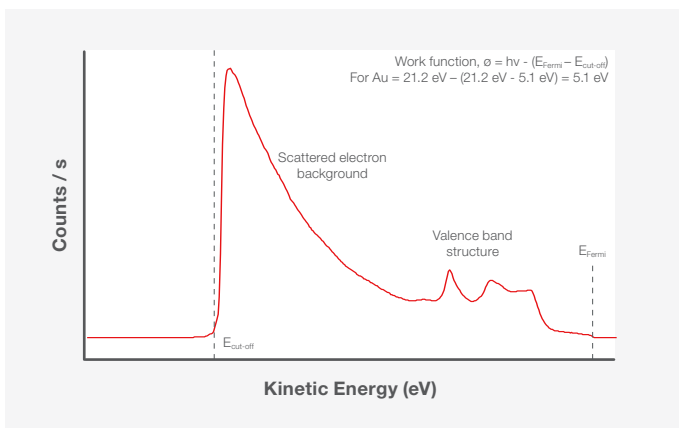


Figure 20. UPS spectrum of cleaned Au sample, with parameters marked for work function measurement.

As a surface property, the work function is strongly influenced by variation in composition or structure at the surface, such as atmospheric contamination. The combination of argon cluster cleaning with UPS, where the clusters can clean the surface without damaging the underlying material, has become particularly useful. Similarly, UPS can be combined with argon sputtering, just like XPS, to enable UPS depth profiling where the work function and valence band structure can be measured as functions of depth. Furthermore, if XPS and UPS are combined together with depth profiling, the user can measure elemental/chemical composition with XPS at the same time as measuring the electronic structure with UPS (see Figure 21).

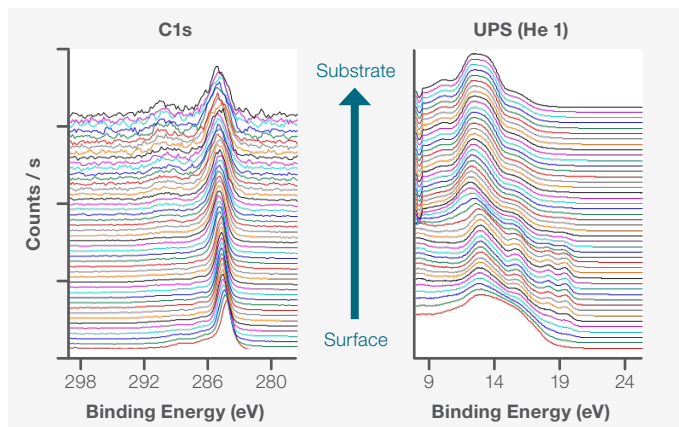
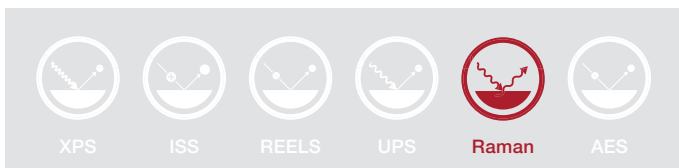


Figure 21. Combined XPS/UPS depth profile of 10 nm C60 on CaF2 substrate.



## Raman spectroscopy

Raman spectroscopy is a technique based on the scattering of laser light from a sample. Much of the incident light is scattered from the sample without changing frequency (Rayleigh scattering), but some of the photons interact with the vibrational states of the molecules in the samples and are scattered with different frequencies. This is called Raman scattering, and it is useful because it can give chemical and structural information about a sample, including molecular identity, film thickness, and concentration of defects. (See Figure 22 for an example of Raman analysis of graphene.)

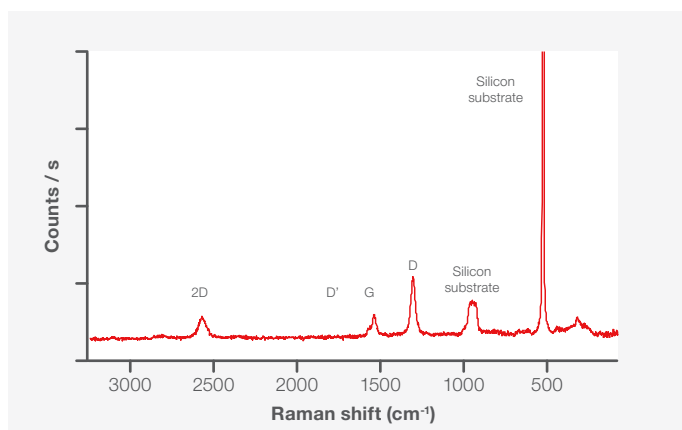


Figure 22. 532nm Raman spectrum of a graphene film on silicon.

XPS is complementary to Raman spectroscopy in a number of different ways. As mentioned previously, XPS is always a surface sensitive technique (0–10 nm), irrespective of the sample being analyzed. In contrast, the sampling depth of Raman spectroscopy varies quite significantly depending on the type of material being analyzed. When analyzing a polymer, for example, Raman is thought of more as a bulk sensitive technique, with a sampling depth on the micron scale. As seen in Figure 22, however, when analyzing 2D materials, such as graphene or MoS<sub>2</sub>, Raman can also give information from films with thicknesses of only one or two molecular layers.

The information provided by XPS is also complementary to Raman spectroscopy (see Figure 23). XPS provides detailed chemical bonding information, based on the shift in core-level energies due to interaction with neighboring atoms. If there was a graphene layer that had been chemically functionalized, with nitrogen or oxygen, for example, XPS would be able to detect the details of carbon-oxygen or carbon-nitrogen bonding. Additionally, not all carbon-containing materials are equally efficient at Raman scattering. If the graphene film has organic residue from the manufacturing process (e.g., PMMA residue), then this will be effectively invisible to Raman spectroscopy, but XPS will be able to detect both the residue and the graphene layer.

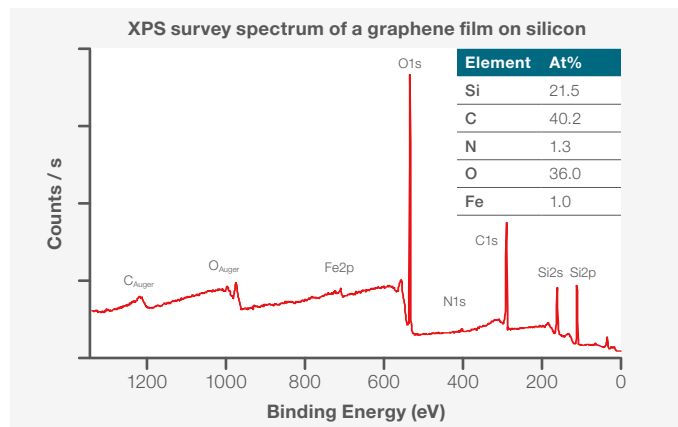
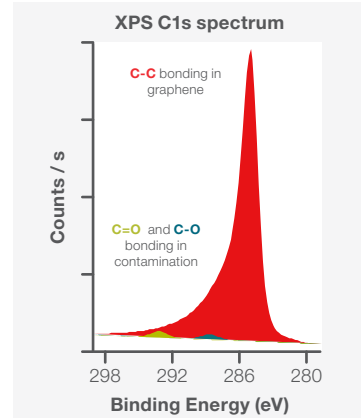
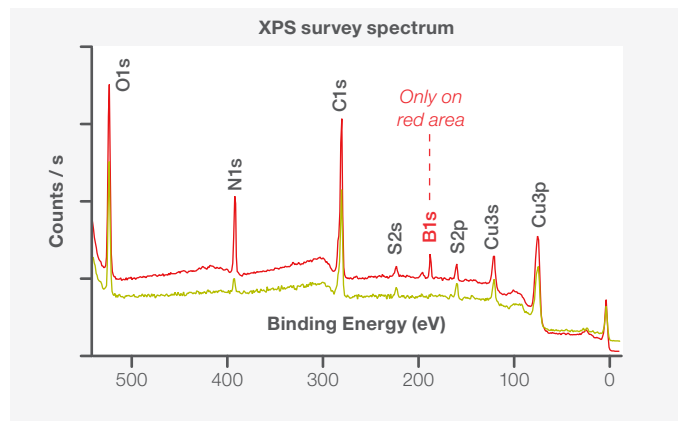
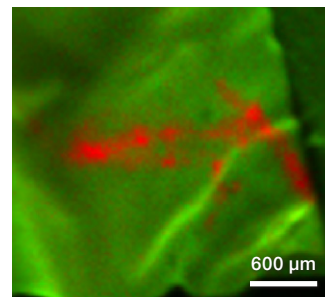


Figure 23. XPS survey scan and C1s scan of a graphene film on silicon.

It has been shown above that XPS and Raman spectroscopy are a useful combination of analytical techniques, giving complementary information. Is it beneficial to have these two techniques together on the same analytical platform or is it reasonable just to have two separate spectrometers for two



different analyses? The Nexsa Surface Analysis System can be configured with both XPS and Raman spectroscopy at the same time. This has proven to be a useful combination with a number of different applications. First, where the features to be analyzed are optically invisible, if the analyst has spent time locating the features on one tool, it may not be possible to find exactly the same feature on a separate tool. The Nexsa System's combination of XPS and Raman allows the same optically invisible feature to be analyzed without moving the sample between analyses. Figure 24 shows an example of this, where a single, optically invisible flake of boron nitride was analyzed with both XPS and Raman at the same time.



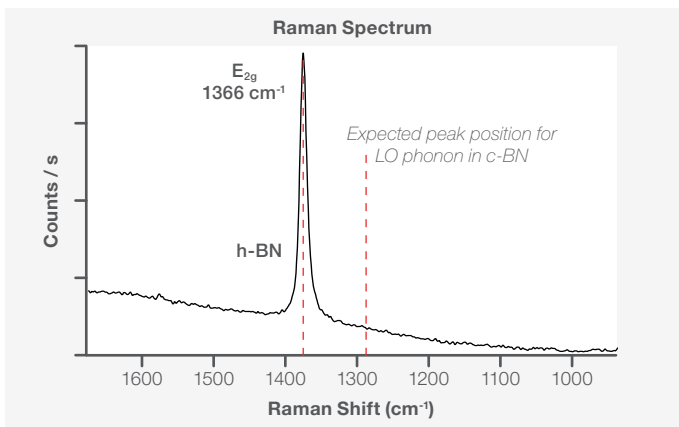


Figure 24. Using XPS SnapMap to locate optically invisible feature, with XPS and Raman analysis at the same location.

The boron nitride film was optically invisible, so rapid XPS mapping (SnapMap) was used to spectroscopically search for the nitride chemical state on the copper substrate. Once the boron nitride area had been found with XPS, it was then possible to acquire XPS survey spectra on/off the nitride and to collect a 532 nm Raman spectrum. The XPS data clearly shows the expected boron and nitrogen signals, but some chlorine contamination was also detected. The Raman analysis revealed the physical structure of the nitride film, showing that it was h-BN (hexagonal) rather than c-BN (cubic).

Other applications for combining XPS and Raman on a single platform involve samples that are atmospherically sensitive and samples that need to be cleaned or depth profiled with an ion gun. An example of the former would be battery material analysis (see Figure 25), where a sample needs to be transferred in the XPS system under an inert atmosphere, and it would then be difficult to take the same sample and move it through the atmosphere to a separate Raman tool.

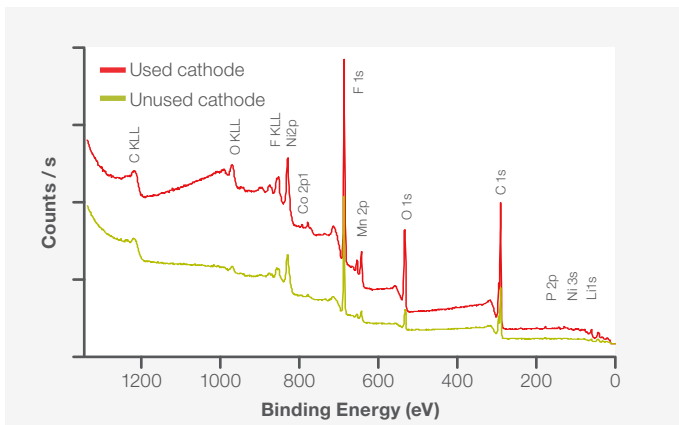


Figure 25. XPS analysis of cathodic materials from a Li-ion battery. Sample transferred into Nexsa Surface Analysis System using Vacuum Transfer Module.

Another example of the need for a combined XPS/Raman analysis on a single platform involved investigation of PMMA residue remaining on graphene after the manufacturing process. As mentioned above, XPS can distinguish easily between carbon bonding in graphene and carbon bonding in organic residue. The aim of the analysis was to use argon clusters to gently remove the residue, leaving behind only graphene. But a question remained. What are the best argon cluster conditions to use (e.g., cluster size, energy) for cleaning but without damaging the structure of the graphene? Raman spectroscopy can detect whether defects have been formed by the ion bombardment, but if the sample is taken out of the XPS system after argon cluster cleaning, the sample could be re-contaminated with carbon material from the atmosphere. Additionally, it may also be difficult to find the optically invisible zone where the ion cleaning occurred. A combined XPS/Raman capability on the same tool allows an argon cluster depth profile to be performed (see Figure 26), where XPS shows changes in the carbon bonding state as a function of depth and Raman can be used to monitor defect creation in the graphene layers. The XPS shows that argon clusters have successfully removed the residue, but the Raman shows that there was a small increase in defects (as shown by the increase in D-band intensity) accompanying the sputtering. It was found that, by reducing the energy and increasing the size of the clusters, the graphene surface was still cleaned while an increase in defect density was prevented.

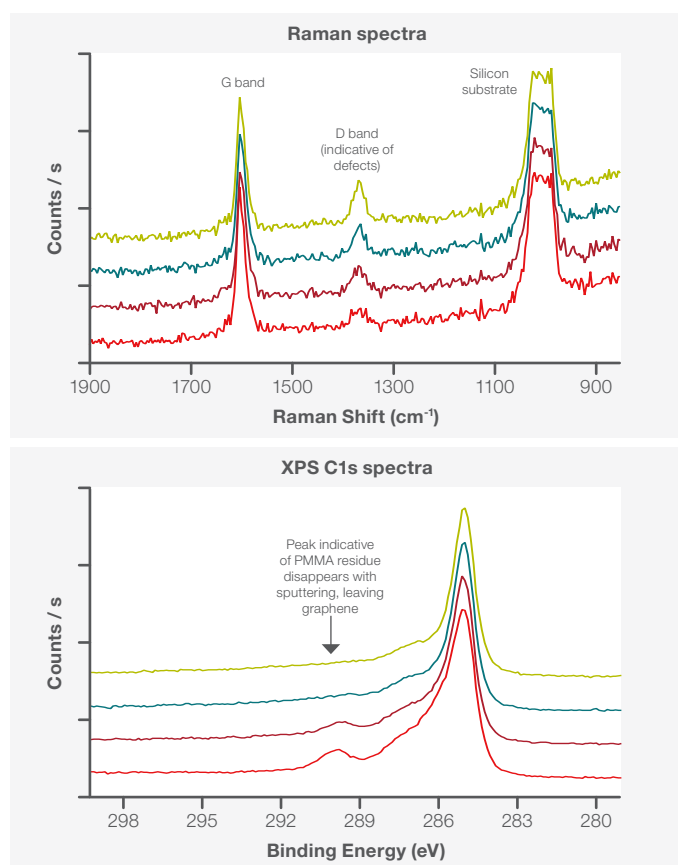
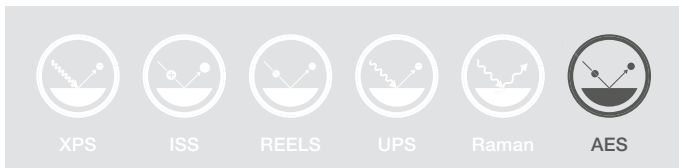


Figure 26. Combined XPS/Raman argon cluster ion depth profile of PMMA residue on graphene.



## Auger electron spectroscopy (AES)

Auger electron spectroscopy (AES) is named after Pierre Auger, who was one of the people who discovered the technique. In AES, the sample is irradiated with a focused beam of electrons instead of the X-rays used in XPS. The electron beam can be focused to a much smaller spot size than X-rays, and this is one of the main reasons for using AES rather than XPS. With AES, the probe spatial resolution can be less than 100 nm, compared to perhaps 10  $\mu\text{m}$  for XPS, and therefore much smaller features can be analyzed.

A schematic of the overall Auger process is shown in Figure 27. When the focused beam of electrons strikes the sample surface, if the beam energy is high enough, electrons are emitted from the core levels of the atoms, similar to photoelectron emission with XPS. The remaining core hole can then be filled by an electron from a higher energy level, and at this point, two competing processes can occur. First, as the higher lying electron fills the core hole, there can be emission of a photon, and this is the process behind energy dispersive X-ray spectroscopy (EDS). Alternatively, instead of radiative relaxation, as the higher lying electron fills the core hole, an additional electron, also from a higher lying level, can be emitted. This is the Auger electron. A sample containing a number of different elements will emit Auger electrons across an entire range of kinetic energies with intensities related to the number of atoms of the elements present. Unlike XPS, where the photoelectron energy depends directly on the energy of the incident photon, the energies of Auger electrons depend only on the sample electronic configuration and not on the energy of the incident electron beam. With Auger spectroscopy, it is only possible to measure the kinetic energy of the electrons, and this cannot be correlated with binding energy information.

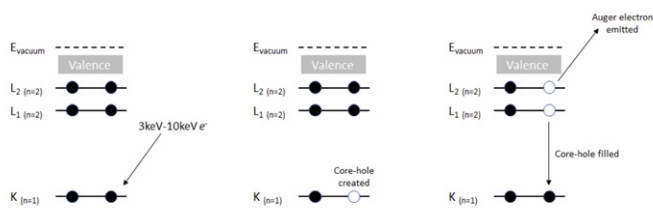


Figure 27. Schematic of the process of Auger electron emission.

An Auger electron spectrometer must therefore consist of a source of energetic electrons (normally from 3–10 keV or higher) and an electron energy analyzer capable of measuring the kinetic energy spectrum, usually up to at least 3 keV. The overall shape of the spectrum, typical of AES, is of a large, decreasing, background of electrons at low kinetic energy followed by a rising background that continues to increase up to the energy of the primary beam. The Auger peaks are superimposed on this background (see Figure 28).

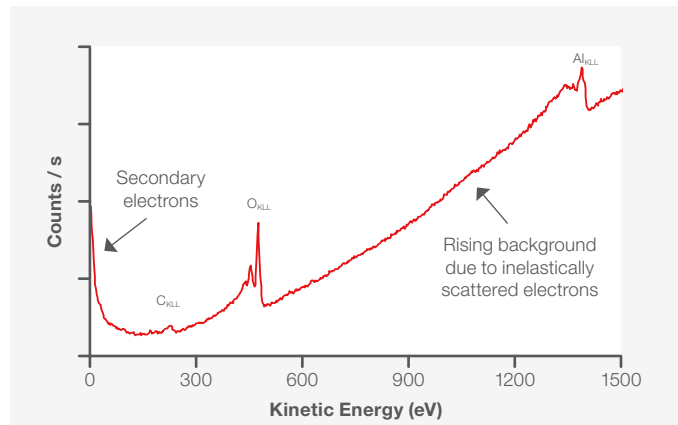


Figure 28. Auger spectrum (integrated version) of oxidized aluminum foil sample.

The Auger process involves three electrons, and the notation used to describe an Auger peak uses the name of the electron shells for all three of them. For the AlKLL peak in Figure 28, the original core hole was made in the K-level (principal quantum number  $n=1$ ), and an electron from the L-level (principal quantum number  $n=2$ ) dropped to fill that core-hole, with concurrent emission of an Auger electron from an orbital in the L-level. (Where the L-levels are also the valence levels, they may sometimes be represented by the letter V, so the KLL peak becomes the KVV peak.) One of the features of Auger spectroscopic peaks is that they form more complex series than observed for XPS. The AlKLL “peak” in Figure 28, for example, is actually composed of several components stretching over a range from 1,300–1,400 eV.

As mentioned above, Auger spectroscopy has the advantage compared to XPS concerning spatial resolution. Auger spectroscopy tends to be more limited, however, concerning chemical bonding state information. For certain elements, such as copper and zinc, Auger spectroscopy is quite rich in chemical information, but with most elements, such as carbon, for example, the information is very limited. An example of a chemically resolved Auger spectrum is shown below in Figure 29. The spectrum is a higher energy resolution version of the AlKLL peaks previously shown in the Auger survey spectrum of Figure 28.

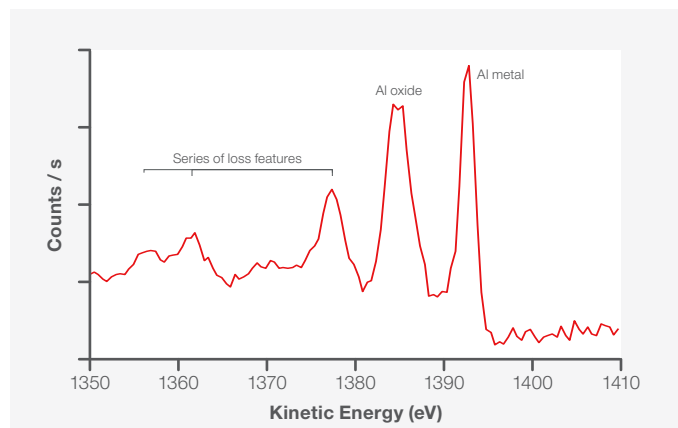


Figure 29. High energy resolution AlKLL spectrum of oxidized Al foil.

Just as with XPS, creation of core-holes and subsequent electron emission during the Auger process can cause charge to build-up on non-conducting surfaces. With XPS, this problem has been effectively solved for many years, typically by using a combination of low-energy electrons and low-energy argon ions to compensate for charge buildup due to photoemission. In Auger spectroscopy, where the probe may be a negatively charged electron beam of several KeV energy and is particularly tightly focused, the charging problem is even more acute on non-conducting samples. Auger charge compensation is possible, but the solution to charging tends to be more variable on a case-by-case basis. Sometimes, simply reducing the beam energy can reduce charging sufficiently, but at other times, it is necessary to flood the surface with low-energy argon ions. The ESCALAB Xi+ XPS Microprobe offers different methods to mitigate charging.

The example below shows SEM images acquired from a polymer-encased microelectronic device (Figure 24) on an ESCALAB Xi+ XPS Microprobe. One of the SEM images (Figure 30a) was collected with no charge compensation attempted, and it is obvious that the image is obscured by severe charging. The other SEM image (Figure 30b) was collected after flooding the surface with low-energy argon ions, and the structure of the microelectronic device is now clear.

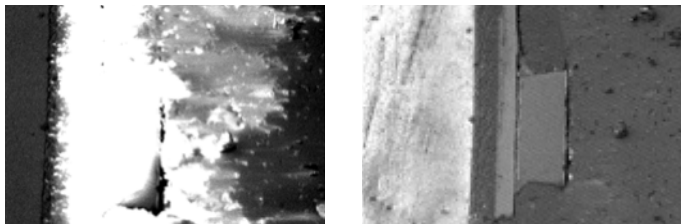


Figure 30. ESCALAB Xi+ XPS Microprobe SEM images collected with/without charge compensation.

Similar to XPS, Auger spectroscopy is not just confined to single point analysis. Auger mapping is a relatively common technique for measuring the spatial distribution of elements on a surface. An ESCALAB Xi+ XPS Microprobe, configured with AES, was used to analyze a rock cross-section that had been mounted on a glass slide (Figure 31). The rock cross-section was insulating, and it was also mounted on an insulating substrate, so it was necessary to use charge compensation tactics to acquire good data.

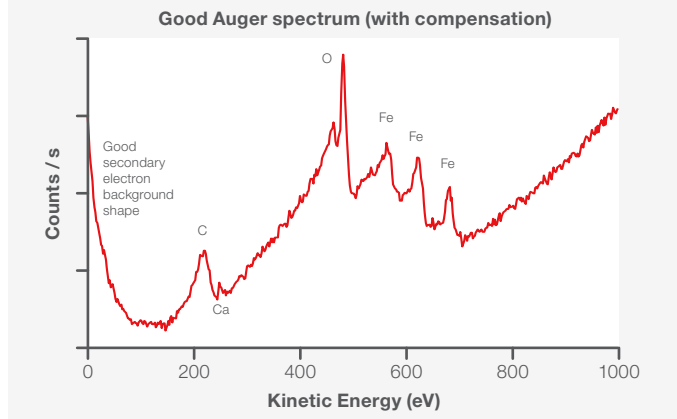
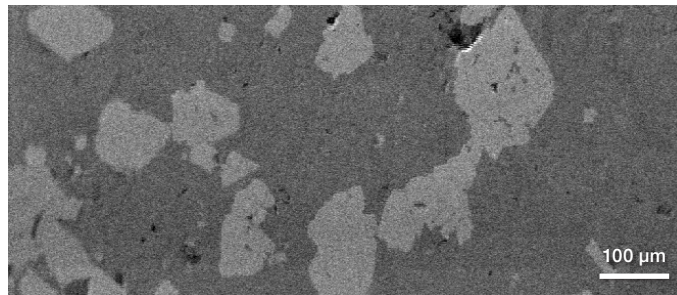
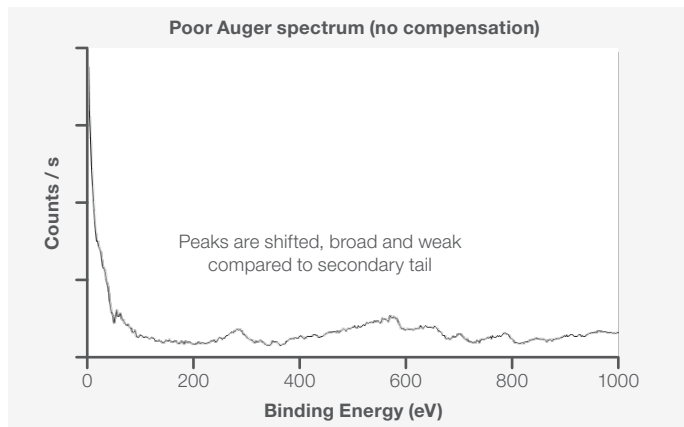
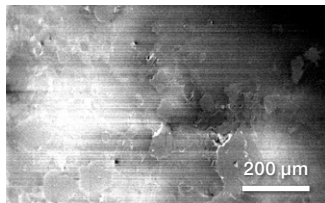


Figure 31. Point analysis on the rock cross-section with/without charge compensation.

After point analysis was performed (Figure 31), a portion of the sample was mapped with Auger electron spectroscopy to establish the distribution of iron across the surface (Figure 32). The iron Auger map nicely shows the potential spatial resolution of AES. (Some of the particles are <1 µm in size). Additionally, where a dark void was identified on the iron Auger map, it is then possible to collect an Auger survey spectrum from that location and establish that there was no iron there.

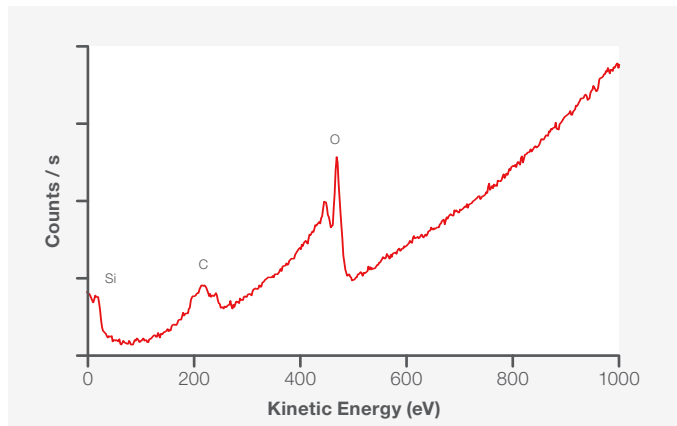
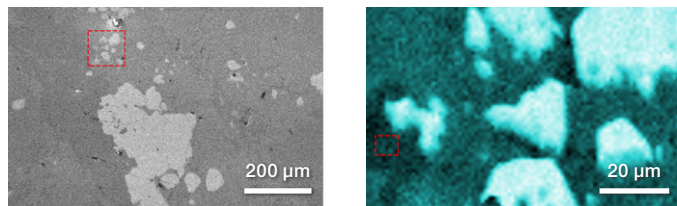


Figure 32. Iron Auger map from area indicated on SEM, together with Auger survey spectrum from dark void in Auger map.



## Summary

X-ray photoelectron spectroscopy (XPS) is a very powerful technique for analyzing the elemental and chemical state composition of surfaces. Even with all of the advantages of the technique, there may still be information required by the analyst that it cannot provide. On Thermo Scientific surface analysis systems (Nexsa System and ESCALAB Xi+ XPS Microprobe), it is possible to combine XPS with one or more complementary analysis techniques on a single platform. With the Nexsa System, for example, XPS can be combined with Raman and reflection electron loss spectroscopy (REELS) to more fully characterize graphene for chemical bonding states, defects, and electronic structure. On the ESCALAB Xi+ XPS Microprobe, Auger can be configured to allow for smaller features to be analyzed than is possible with XPS alone. The multi-technique possibilities offered by Thermo Scientific systems opens the way for a more complete analysis of your samples.



Find out more at [thermofisher.com/xps](https://thermofisher.com/xps)

**ThermoFisher**  
SCIENTIFIC